

Subvolume method for SU(2) Yang-Mills theory at finite temperature: topological charge distributions

Norikazu Yamada,^{a,b} Masahito Yamazaki,^{c,d,e} Ryuichiro Kitano^{a,b}

^a*High Energy Accelerator Research Organization (KEK), Tsukuba 305-0801, Japan*

^b*Graduate University for Advanced Studies (SOKENDAI), Tsukuba 305-0801, Japan*

^c*Kavli Institute for the Physics and Mathematics of the Universe (WPI), University of Tokyo, Kashiwa, Chiba 277-8583, Japan*

^d*Center for Data-Driven Discovery, Kavli IPMU (WPI), University of Tokyo, Kashiwa, Chiba 277-8583, Japan*

^e*Trans-Scale Quantum Science Institute, The University of Tokyo, Tokyo 113-0033, Japan*

E-mail: norikazu.yamada@kek.jp, masahito.yamazaki@ipmu.jp,
ryuichiro.kitano@kek.jp

ABSTRACT: We apply the previously-developed sub-volume method to study the θ -dependence of the four-dimensional SU(2) Yang-Mills theory at finite temperature. We calculate the first two coefficients, the topological susceptibility χ and the fourth cumulant b_2 , in the θ -expansion of the free energy density around the critical temperature (T_c) for the confinement-deconfinement transition. Lattice calculations are performed with three different spatial sizes $24^3, 32^3, 48^3$ to monitor finite size effects, while the temporal size is fixed to be 8. The systematic uncertainty associated with the sub-volume extrapolation is studied with special care. The sub-volume method allows us to determine the values of b_2 much more accurately than the standard full-volume method, and we successfully identify the temperature dependence of b_2 around T_c . Our numerical results suggest that the θ -dependence of the free energy density near $\theta = 0$ changes from $4\chi(1 - \cos(\theta/2))$ to $\chi(1 - \cos \theta)$ as the temperature crosses T_c .

Contents

1	Introduction	1
2	Lattice set-up and methods	2
2.1	Lattice parameters	2
2.2	Topological charge density on the lattice	3
2.3	Sub-volume method	3
3	Numerical results	5
3.1	Sub-volume extrapolation	5
3.2	Extrapolation to $n_{\text{APE}} = 0$	5
3.3	Main results	5
4	Comments on uncertainties in the large sub-volume extrapolation	10
5	b_2 in the confined phase	11
6	Summary	12

1 Introduction

It has been a long-standing problem to identify the effect of the θ parameter [1] on the dynamics of four-dimensional pure $\text{SU}(N_c)$ Yang-Mills (YM) theory. The problem can be further enriched by considering the theory at finite temperature T .

While there have been attempts to study the θ - T phase diagram, the previous studies were restricted to limited regions of it. Along the temperature axis (*i.e.* $\theta = 0$), the existence of the confinement-deconfinement phase transition has been well established, and the critical temperature (T_c) and other properties of the phase transition were explicitly determined on the lattice for some theories [2, 3]. It is also possible to explore the small- θ region by various techniques, such as reweighting, Taylor expansion in θ , or analytic continuation into imaginary θ [4–13].

Recently a novel analysis method, called *the sub-volume method*, was developed in [14] to investigate the region $\theta \sim O(1)$ for the pure $\text{SU}(2)$ YM theory at zero and finite temperatures¹. The result suggests spontaneous CP violation at $\theta = \pi$ in the vacuum and the restoration above T_c , thus qualitatively the same picture as the large N_c limit [15–18] emerges; see also [19–25] for samples of related analysis for finite N_c pure YM theory.

In this paper we study the θ dependence of the free energy density of the pure $\text{SU}(2)$ YM theory near the critical temperature, where the free energy density is expected to

¹The $\theta \sim O(1)$ region is explored also in [12] relying on analytic continuation.

undergo a qualitative change. We determine the first two coefficients appearing in the Taylor expansion of the free energy density, the topological susceptibility χ and the fourth cumulant b_2 . While the lattice determinations of these quantities across T_c are available for $N_c \geq 3$ in [4, 10], little has been done in $N_c = 2$ except for [26]. Furthermore, the determinations of χ and especially b_2 require high statistics. Indeed, $O(100,000)$ configurations had to be accumulated to reach a reasonable accuracy for the calculation of b_2 in SU(2) YM theory at $T = 0$ [5]. The situation, however, is significantly improved in the newly-proposed sub-volume method [14] as described below. The basic idea of the sub-volume method is inspired by the work of [27] done in two dimensions. The slab method [28–30] and the method using the sub-volume introduced in [31] were proposed to resolve the problem of frozen topology and are conceptually different from but operationally similar to ours.

The rest of this paper is organized as follows. The lattice setup and parameters are summarized in sec. 2, which also includes the definition of the local topological charge on the lattice as well as the explanation of the sub-volume method. In sec. 3, we present our main results and discuss the detailed numerical analysis step by step. The sub-volume method has a subtlety in the estimate of uncertainties associated with the large sub-volume extrapolations. Section 4 is devoted to the discussion of this uncertainty. Motivated by the numerical results obtained here, we conclude that b_2 is approximately independent of T in the confined phase and infer the whole θ -dependence of the free energy density below T_c in sec. 5. Finally, the study is summarized in sec. 6.

2 Lattice set-up and methods

2.1 Lattice parameters

The SU(2) lattice gauge action at $\theta = 0$ is described by

$$S_g = 6\beta N_{\text{full}} \{c_0(1 - W_P) + 2c_1(1 - W_R)\} , \quad (2.1)$$

where $\beta = 4/g^2$ is the inverse lattice gauge coupling. The 1×1 plaquette and the 1×2 rectangle are constructed from SU(2) link variables, and W_P and W_R are those averaged over four dimensional lattice sites ($N_{\text{full}} = N_S^3 \times N_T$) and all possible directions, respectively. The coefficients c_0 and c_1 satisfying $c_0 = 1 - 8c_1$ are the improvement coefficients, and we take the tree-level Symanzik improved action, $c_1 = -1/12$ [32]. To monitor the stability of numerical results, the calculations are carried out on three lattice sizes ($N_S = 24, 32, 48$) with $N_T = 8$ fixed. The critical value of β at $\theta = 0$ for $N_T = 8$, corresponding to the critical temperature T_c , is known to be $\beta_c = 1.920(5)$ [33, 34], around which we perform the numerical simulations.

Gauge configurations are generated by the Hybrid Monte Carlo method with periodic boundary conditions in all directions, and stored in every ten trajectories after thermalization. Statistical errors are estimated by the single-elimination jack-knife method with the bin size of 1,000 configurations. Simulation parameters including the lattice size and the statistics are summarized in Tab. 1.

β	1.80	1.85	1.86	1.87	1.88	1.89	1.90	1.91	1.92	1.93	1.94	1.95	2.00
T/T_c	0.68	0.80	0.83	0.85	0.88	0.91	0.94	0.97	1.00	1.03		1.10	1.30
$N_S=24$			30	30	20	20	20	32	50	20			
32	30	30	10	20	40	30	30	54	50	50	50	31	10
48	25			10		20	20	30	38	12		12	10

Table 1. The simulation parameters and statistics. The numbers of configurations are shown in units of 1,000. The temporal size N_T is fixed to 8. The normalized temperature T/T_c is obtained by fitting the data presented in [34].

2.2 Topological charge density on the lattice

The sub-volume method, described in the next subsection, requires the local values of the topological charge density. The conceptually cleanest way to measure them would be to use the eigenvectors of the overlap Dirac operator [35]. However, this method is not realistic for high-statistics and large-volume lattice calculations because the computational cost is too large. Instead, we use the bosonic definition, where the topological term $G\tilde{G}$ is directly constructed from the $SU(2)$ link variables. The topological charge distribution thus obtained is distorted by lattice artifacts, which need to be eliminated by the smearing procedure. The smearing, however, may simultaneously deform physically legitimate topological excitations. Based on the study of this point in [5], we estimate the physical topological quantities by extrapolating the smeared data over a suitable range of the smearing steps to the zero smearing.

Among several mutually-consistent methods often used in the literature [36–38], we choose the APE smearing [39] and the five-loop improved topological charge operator [40] to calculate the local topological charge $q(x, n_{\text{APE}})$ on each configuration. This procedure and the parameters for the APE smearings are precisely the same as those used in [5, 14].

A local topological charge is calculated at every five smearing steps, *i.e.* $n_{\text{APE}} = 0, 5, 10, \dots, 50$ and is uniformly shifted as $q(x, n_{\text{APE}}) \rightarrow q(x, n_{\text{APE}}) + \epsilon$ such that the global topological charge $Q_{\text{full}} := \sum_{x \in N_{\text{full}}} q(x, n_{\text{APE}})$ takes the integer value closest to the original one.

Figure 1 shows the histograms of global topological charge Q_{full} thus obtained at $n_{\text{APE}} = 30$. It is seen that topology fluctuates appropriately for all the values of β and N_S studied in this paper.

2.3 Sub-volume method

To study of the θ -dependence of the free energy density $f(\theta)$, we consider the Taylor expansion around $\theta = 0$,

$$f(\theta) = \frac{\chi\theta^2}{2}(1 + b_2\theta^2 + \dots). \quad (2.2)$$

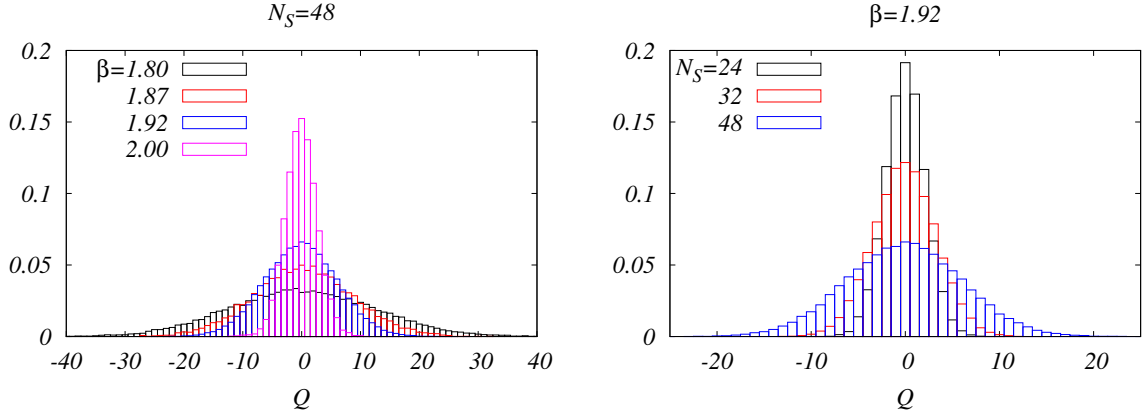


Figure 1. Histogram of global topological charge, Q_{full} , at $n_{\text{APE}} = 30$ at various temperatures (or β) on $N_S = 48$ lattice (left) and at T_c (or β_c) on three different N_S lattices (right).

In the sub-volume method, the first two coefficients χ and b_2 are obtained as

$$\chi_{\text{sub}} = \lim_{n_{\text{APE}} \rightarrow 0} \lim_{l \rightarrow \infty} \chi_{\text{sub}}(n_{\text{APE}}, l) = \lim_{n_{\text{APE}} \rightarrow 0} \lim_{l \rightarrow \infty} \frac{1}{N_{\text{sub}}} \langle Q_{\text{sub}}^2(n_{\text{APE}}) \rangle, \quad (2.3)$$

$$b_{2,\text{sub}} = \lim_{n_{\text{APE}} \rightarrow 0} \lim_{l \rightarrow \infty} b_{2,\text{sub}}(n_{\text{APE}}, l) = \lim_{n_{\text{APE}} \rightarrow 0} \lim_{l \rightarrow \infty} \frac{-\langle Q_{\text{sub}}^4(n_{\text{APE}}) \rangle + 3 \langle Q_{\text{sub}}^2(n_{\text{APE}}) \rangle^2}{12 \langle Q_{\text{sub}}^2(n_{\text{APE}}) \rangle}, \quad (2.4)$$

where

$$Q_{\text{sub}}(n_{\text{APE}}) := \sum_{x \in N_{\text{sub}}} q(x, n_{\text{APE}}). \quad (2.5)$$

and the sub-volume sizes are $N_{\text{sub}} = l^3 \times 8$ with $l = 8, 12, 16, \dots, N_S$. We have taken full advantage of the translational invariance and hence the results from smaller sub-volumes are statistically more accurate. While we can exchange the order of the $n_{\text{APE}} \rightarrow 0$ limit and the large sub-volume limit $l \rightarrow \infty$, we have chosen the ordering as above which gives slightly better statistical uncertainties.

As pointed out in [14], the sizes of sub-volume (or l) used in the large sub-volume extrapolation have to be carefully chosen, and the suitable range is not known in advance. A reasonable choice for the lower end of the range would be $l_{\text{min}} = N_T$, which corresponds to $1/T$ in physical unit. On the other hand, the upper end has to be chosen such that the sub-volume does not see the boundary of the lattice. It seems reasonable to set $l_{\text{max}} \leq N_S/2$. We will decide l_{max} by comparing the data from three lattices with different N_S 's.

In the above expression, replacing Q_{sub} and N_{sub} with Q_{full} and N_{full} respectively ends up with the standard method using the full-volume data. We denote the resulting values of χ and b_2 by χ_{full} and $b_{2,\text{full}}$, respectively.

3 Numerical results

3.1 Sub-volume extrapolation

We calculate χ_{sub} and $b_{2,\text{sub}}$ following (2.3) and (2.4), respectively. Figure 2 shows the sub-volume (precisely $1/l$) dependence of $\chi_{\text{sub}}(n_{\text{APE}}, l)$ and $b_{2,\text{sub}}(n_{\text{APE}}, l)$, obtained for various ensembles. The data at $n_{\text{APE}} = 30$ are shown as an example. It is seen that for both quantities the data obtained with different N_S are well consistent with each other within uncertainties as long as $l \lesssim N_S/2$. Moreover, the statistical errors of $b_{2,\text{sub}}$ grow more rapidly than those of χ_{sub} as l approaches N_S .

As a general tendency, the deviation among different N_S 's starts to appear in the data on smaller lattice. This is because the sub-volume starts to be affected by the boundary of the lattice when $l \gtrsim N_S/2$. Note that when $l = N_S$ the sub-volume method is nothing but the full volume method under the periodic boundary condition.

In either plots, there is a range of l for which the data on the two largest N_S lattices are consistent. We choose the fit range in the large-sub-volume extrapolation to be $l = [8, 16]$ for all cases, and omit the results with $N_S = 24$ from the main analysis.

Within the fit range, the data are not aligned in a straight line especially for $b_{2,\text{sub}}$, and hence we chose to extrapolate by a quadratic function in $1/l$. To estimate the size of the systematic uncertainty associated with the extrapolation, we also performed a linear extrapolation using two data points at $l = 12$ and 16 . The results of the extrapolations with quadratic and linear functions are shown by solid curves and dotted lines in Figs. 2, respectively.

3.2 Extrapolation to $n_{\text{APE}} = 0$

Next, the data in the large-sub-volume limit obtained at various values of n_{APE} are collected and extrapolated to $n_{\text{APE}} = 0$. In Figs. 3 and 4, the extrapolations of χ and b_2 are shown respectively, where the data from the sub- (left) and the full-volume (right) methods are compared. In the plots for the sub-volume calculations (left), we only show the results from the quadratic extrapolation in $1/l$ for clarity. The data plotted in the full-volume calculations (right) are those obtained at $l = N_S$ without any volume extrapolation. Since n_{APE} dependence is mild, the extrapolation is performed linearly with the fit range of $n_{\text{APE}} = [25, 45]$ in all cases. A different choice of the fit range, for example $n_{\text{APE}} = [20, 40]$, gives only negligible difference.

We choose the same vertical scales on the left and right plots. By comparing the those plots, we find that the statistical uncertainty in the sub-volume method is slightly smaller for χ and significantly smaller for b_2 than those from the full-volume method.

3.3 Main results

After two limiting procedures, we obtain χ and b_2 over the values of β and N_S we have explored. We now try to identify the temperature dependence of these quantities obtained in the sub- and full-volume methods. The T -dependence of χ/T_c^4 and b_2 for $N_S = 32$ and 48 are shown in Fig. 5. In the plot, the central value at each point is defined by the

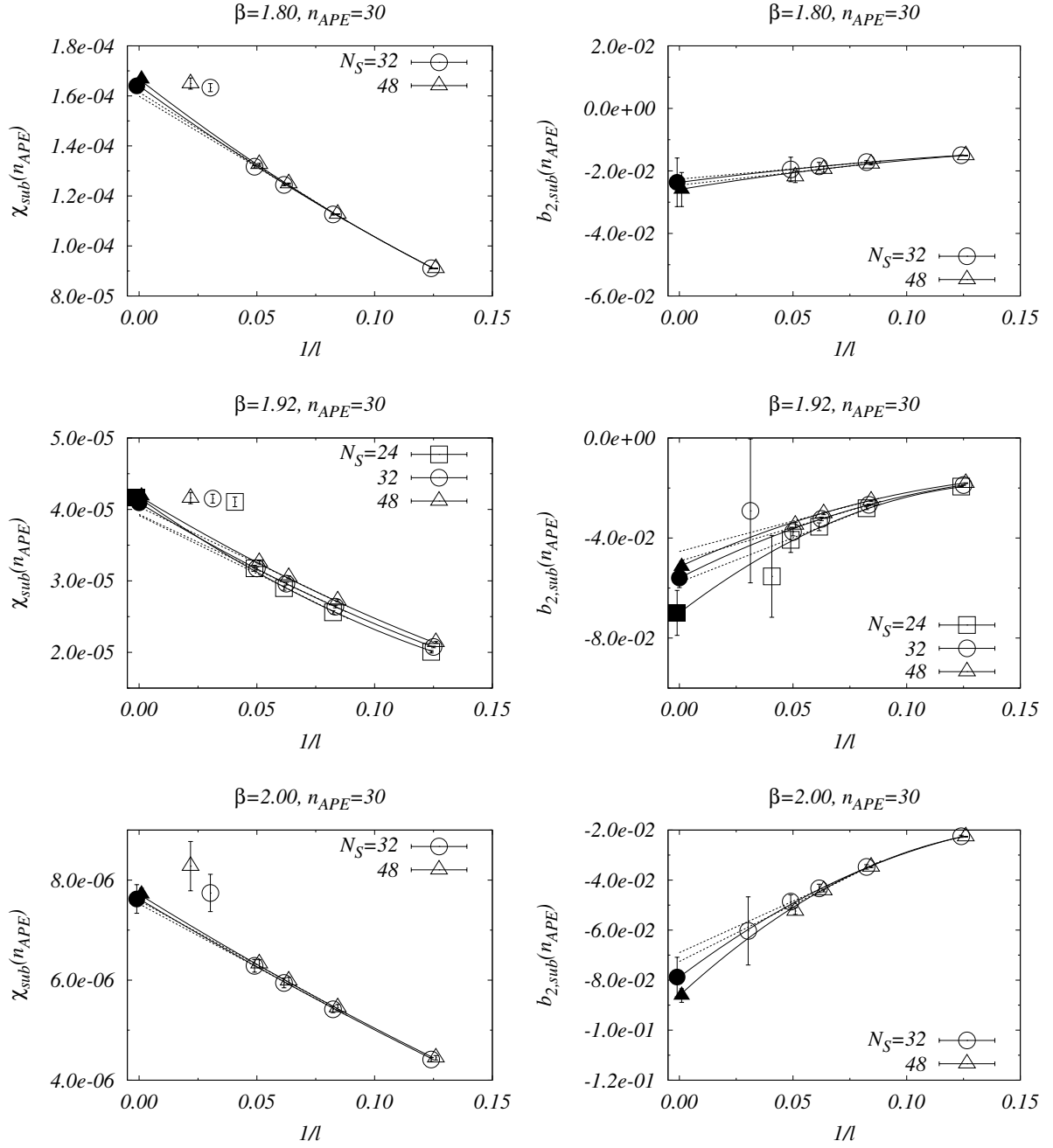


Figure 2. The sub-volume dependence of χ_{sub} and $b_{2,\text{sub}}$. The quadratic (solid) and linear (dotted) extrapolations to the large sub-volume limit are shown.

average of the results with the quadratic and linear extrapolations in $1/l$, and the half of their difference is assigned to the systematic uncertainty². The inner and outer error bars in the sub-volume results represent the statistical error and the sum of the statistical and

²For further discussion on the systematic uncertainty, see the next subsection.

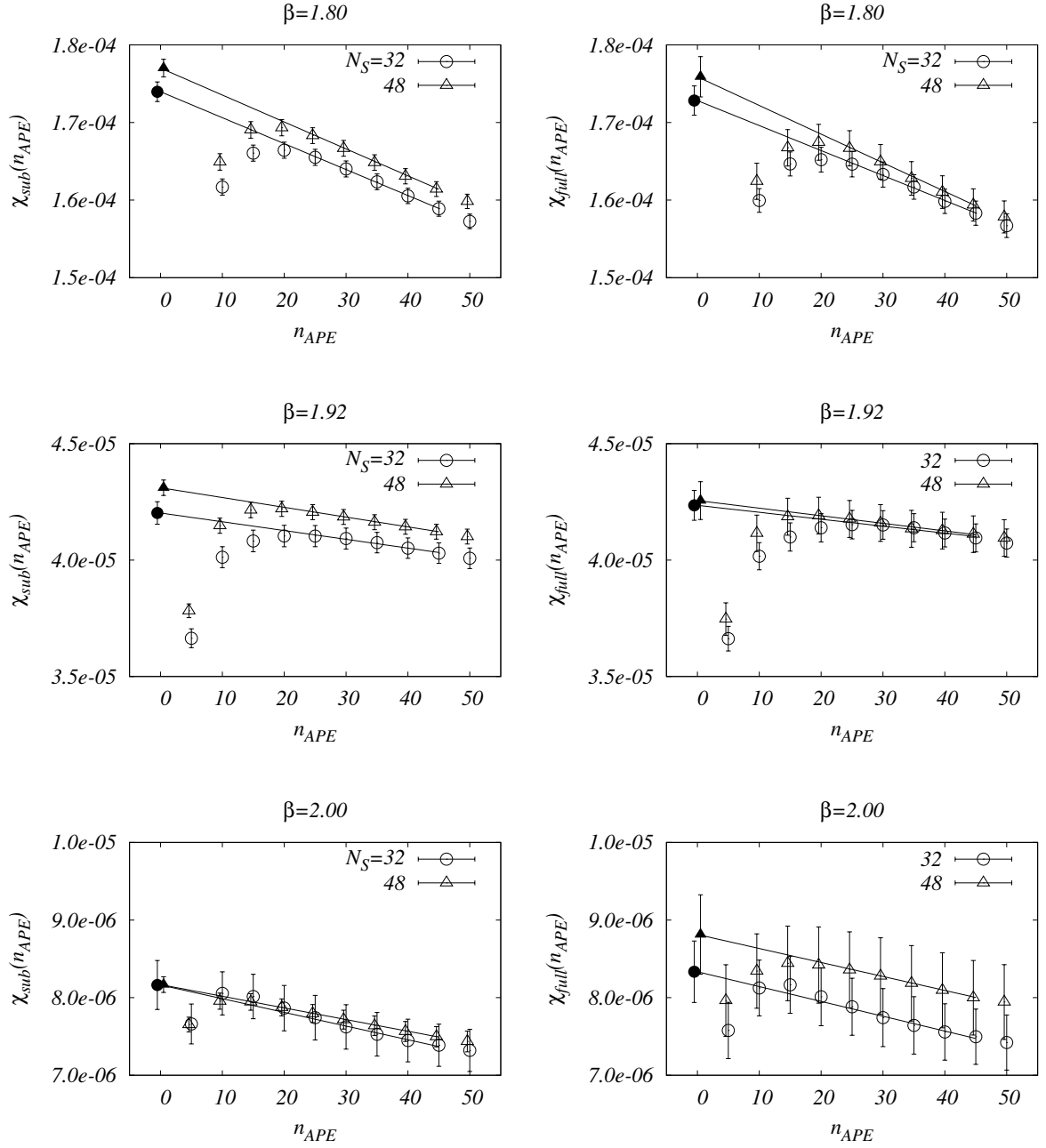


Figure 3. The n_{APE} dependence of χ obtained with sub- (left) and full-volume (right) methods. Linear extrapolations to $n_{APE} = 0$ are also shown (solid lines).

systematic ones, respectively. It is seen that the systematic error for $b_{2,\text{sub}}$ is relatively large at higher T , which reflects a large curvature in the $1/l$ dependence of $b_{2,\text{sub}}$ at such temperatures.

For the T -dependence of χ , the results from the sub- and full-volume are in good

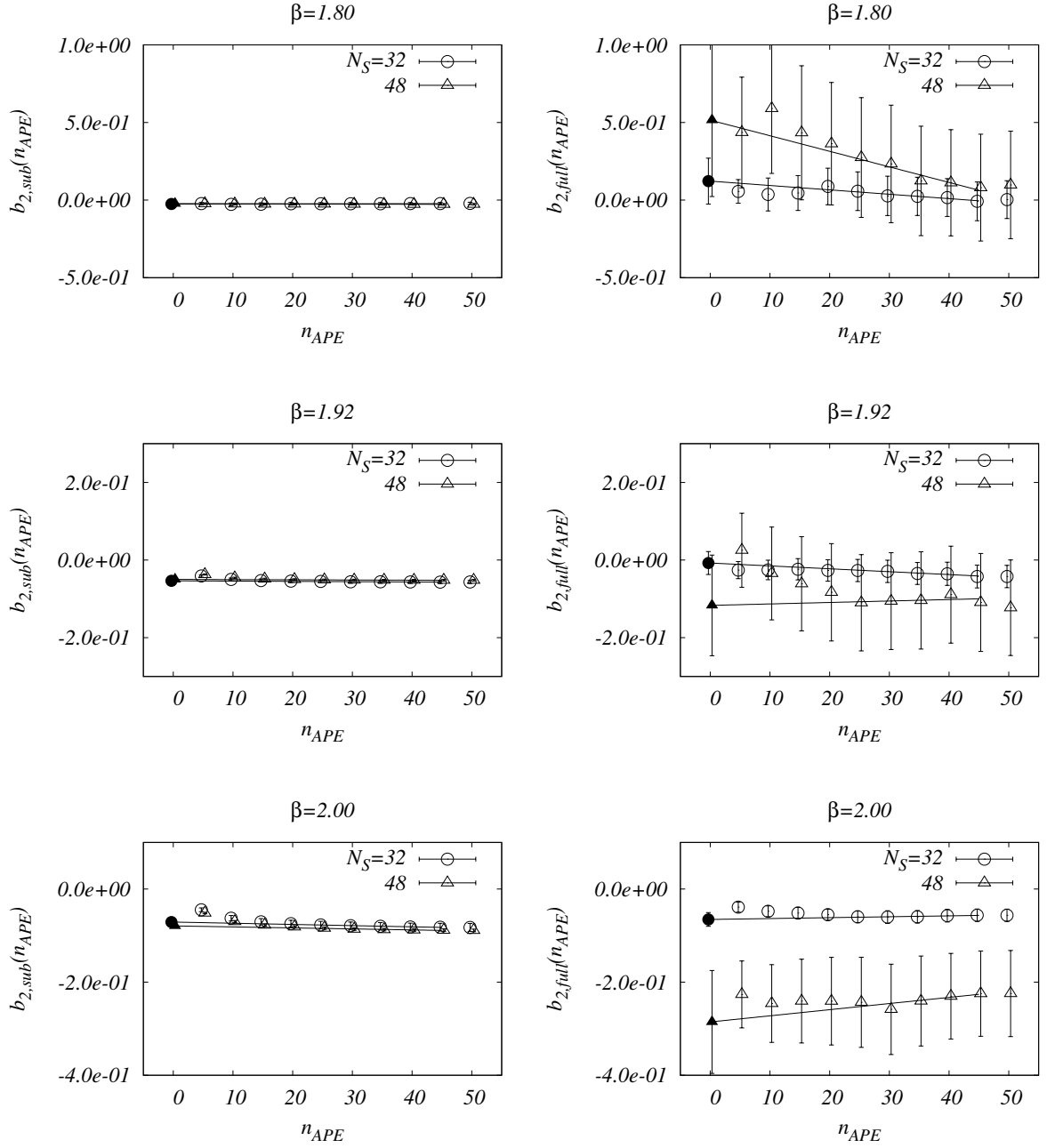


Figure 4. The n_{APE} dependence of b_2 obtained with sub- (left) and full-volume (right) methods. Linear extrapolations to $n_{APE} = 0$ are also shown (solid lines).

agreement, and those with $N_S = 32$ and 48 are also mutually consistent. We hence conclude that the finite size effects are under control. These consistency strongly supports the validity of our procedure of the large-sub-volume extrapolation including the choice of the functional form and the fit range.

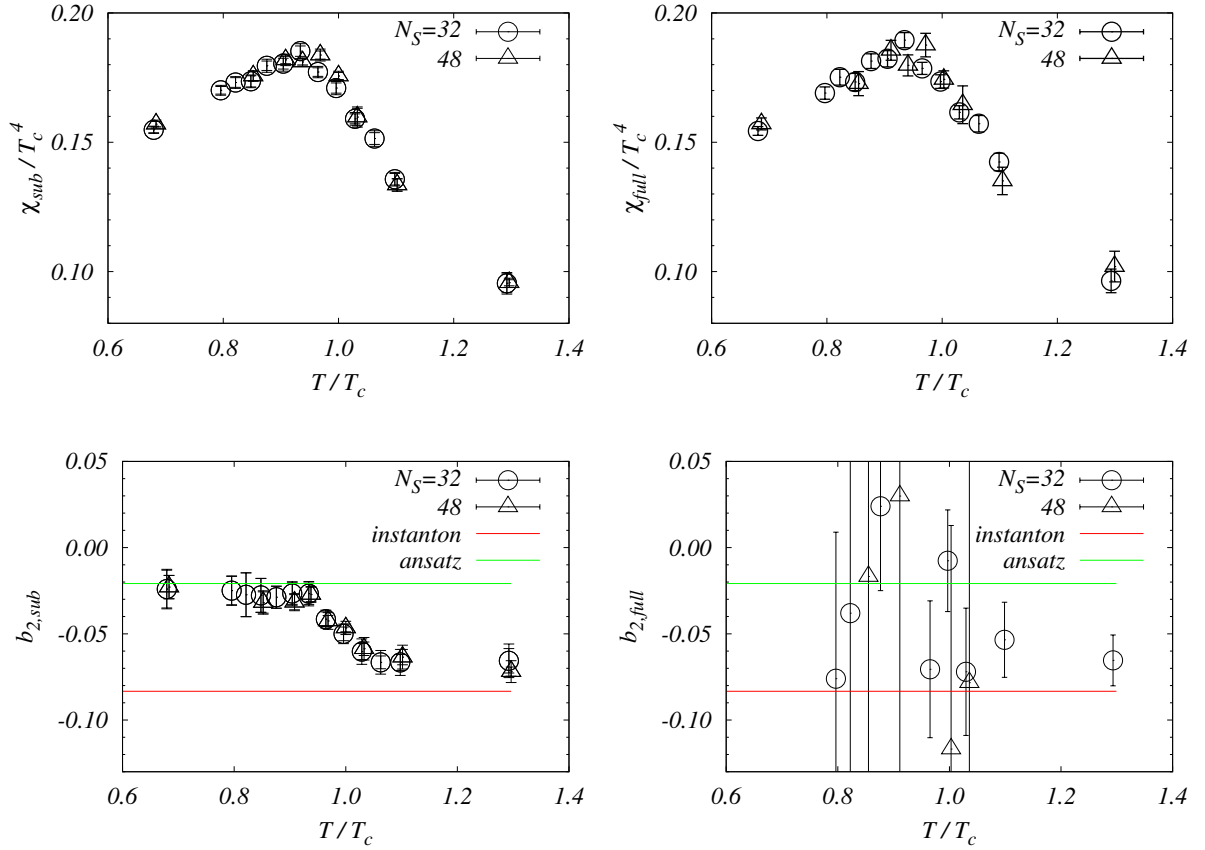


Figure 5. Temperature dependence of χ/T_c^4 and b_2 with the sub-volume (left) and full-volume (right) method. The instanton prediction $b_2 = -1/12$ and a phenomenological ansatz $b_2 = -1/48$ are shown by horizontal lines.

In the SU(3) case, χ is almost a constant below T_c and experiences a gap at T_c before steadily decreasing above T_c to follow the instanton prediction (see, for example, [6, 7, 9–11, 41]). In the SU(2) case, a mild peak is observed slightly below T_c , and no gap exists at $T = T_c$. We suspect that this nontrivial T -dependence originates from the temperature dependence of the glueball mass [42]. While at $T = 0$ the lightest glueball is known to have a mass much larger than the dynamical scale $\Lambda \sim T_c$, it needs to be massless at $T = T_c$ since the phase transition is second-order. Thus it seems reasonable to imagine that at slightly below T_c light glueballs contribute to the free energy, thereby yielding a nontrivial T -dependence of χ . Such a temperature-dependence of the glueball mass has not been reported in the literature, and hence it is interesting to study the dependence and compare the SU(2) case with other SU(N_c) theories.

For the subleading coefficient b_2 , the statistical error is improved remarkably in the sub-volume method, and this has led to a clear demonstration of its temperature dependence. The data above T_c are close to the value $b_2 = -1/12$ (shown as one of the horizontal lines) as predicted by the dilute instanton calculus [43], and we expect b_2 to further approach the

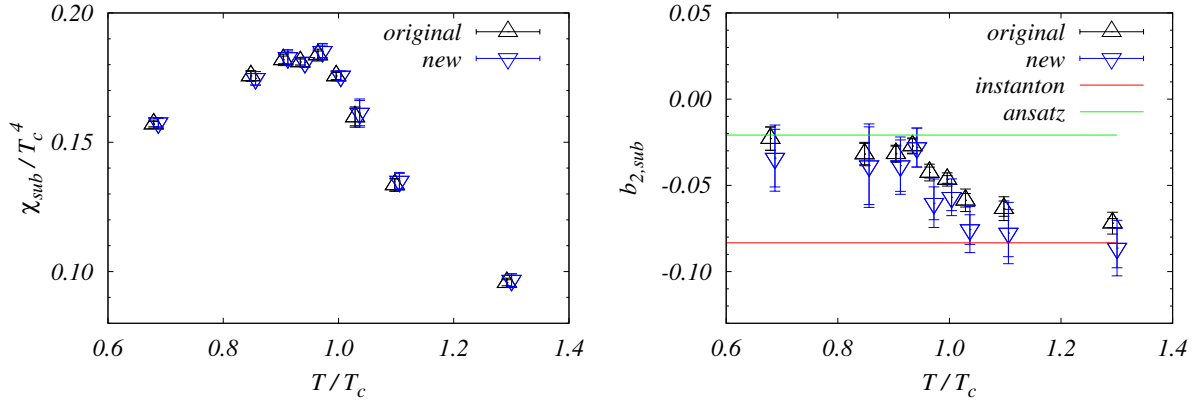


Figure 6. T dependence of χ/T_c^4 (left) and b_2 (right) from the sub-volume method on $48^3 \times 8$. The results with the original and new fit ranges are compared.

instanton prediction as one goes to higher temperature. Below $0.95 T_c$, b_2 again appears to be T -independent and consistent with the value $-1/48$, which is shown as another horizontal line. We discuss the possible origin of this value in the next section.

The T -dependence of b_2 is qualitatively similar to the SU(3) case except around the transition region, where a negative peak is observed in SU(3) [10]. It is interesting to see how the different T -dependence of b_2 is produced by the different nature of the phase transitions.

4 Comments on uncertainties in the large sub-volume extrapolation

The sub-volume method has a subtlety in the extrapolation of the sub-volume data to the large volume limit because the data with $l \gtrsim N_S/2$ can not be used in the extrapolation. Thus, special care has to be paid to the estimate of the systematic uncertainty associated with the subvolume extrapolations. As described above, we have tried to see the systematic uncertainty in several different ways by 1) performing the linear and quadratic extrapolations, 2) comparing the results from different N_S and 3) comparing with the full volume results if available. In order to further explore the uncertainty, 4) the fit range in the extrapolation is varied. We shift the fit range towards larger l (to be explicit, from $l = [8, 16]$ to $l = [12, 20]$) and repeat the same analysis. Since we would like to keep $l < N_S/2$ to avoid the boundary effects, the analysis with the new fit range is possible only on $48^3 \times 8$ lattices.

Figure 6 shows the comparison of the result with the original and new fit ranges both obtained with $N_S = 48$. For χ , no difference is observed between two fit ranges, and the estimate of the systematic error is validated. It is seen for b_2 that, while the two fit ranges result in consistent values and the T dependence, the large statistical errors in the new results make the difference caused by the different fit ranges ambiguous. Although our

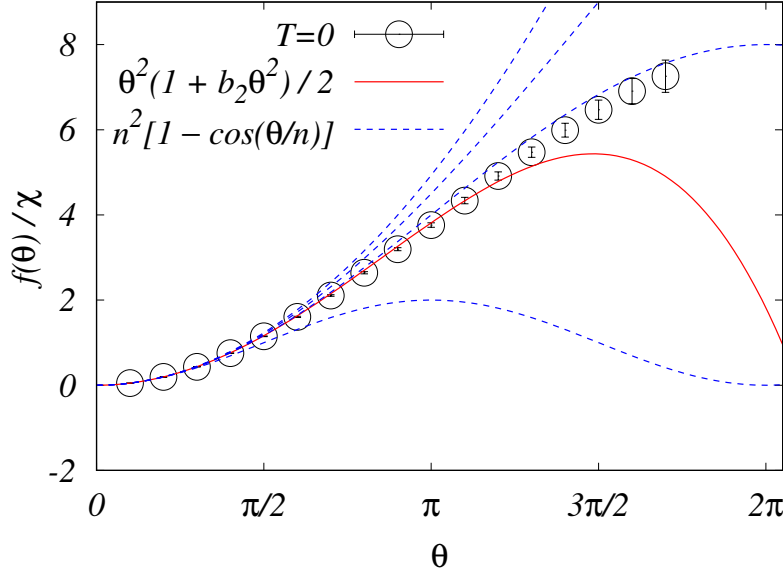


Figure 7. The θ -dependence of the free energy density at $T = 0$ [14]. The curves shown are $\theta^2(1 + b_2\theta^2)/2$ with $b_2 = -0.023$ (solid) and $n^2(1 - \cos(\theta/n))$ with $n = 1, 2, 3, \infty$ from bottom to top (dashed).

calculation does not aim at the accurate determination of b_2 , the conservative estimate of the error should take into consideration the spread observed in Figure 6.

5 b_2 in the confined phase

In the previous section, we have seen that b_2 is almost T -independent separately in the confined and deconfined phases. While in the deconfined phase the observed asymptotic value $b_2 = -1/12$ is expected from the instanton calculus and asymptotic freedom, there is no obvious explanation for the value in the confined phase. Below we speculate on the reason for the observed constant value of b_2 in the low T phase.

Assuming that $b_2 = -0.023(7)$ obtained at our lowest temperature is valid even down to $T = 0$, we compare the curve $f(\theta)/\chi = \theta^2(1 + b_2\theta^2)/2$ with the numerical results for the vacuum energy density calculated in [14]. In Fig. 7, one finds that the curve well describes the numerical results up to around $\theta \sim \pi$. To eliminate the discrepancy for $\theta > \pi$, we further assume that a branch of the vacuum energy density $f(\theta)$ has a periodicity of $2n\pi$ in θ , where n is an unknown natural number. One of the simplest possibilities is $f(\theta)/\chi = n^2(1 - \cos(\theta/n))$, where the overall factor is chosen such that its Taylor expansion reproduces (2.2). $n = 1$ corresponds to the instanton prediction realized in the deconfined phase. To find the best value of n , $n^2(1 - \cos(\theta/n))$ is drawn for $n = 1, 2, 3, \infty$ in the same plot. We find that the discrepancy is minimum at $n = 2$, which corresponds to $b_2 = -1/48 \approx 0.021$.

In the plot of $b_{2,\text{sub}}$ in Fig. 5, a horizontal line has been drawn at $b_2 = -1/48$. The agreement of the data and $-1/48$ is remarkable below $0.95 T_c$. From this observation, it is natural to deduce that the θ -dependence of the free energy density, normalized by the topological susceptibility, is approximately $4(1 - \cos(\theta/2))$ in the confined phase and $1 - \cos \theta$ in the deconfined phase at least in the vicinity of $\theta = 0$.

In [5], b_2 of SU(2) YM is calculated at $T = 0$ in the full-volume method, and collecting the results of b_2 from other SU(N_c) theories [8, 44], the authors tested whether the $N_c = 2$ theory is large N_c -like or instanton-like, *i.e.* $b_2 \sim 1/N_c^2$ or $-1/12$. While the conclusion was against the instanton-like, it was difficult to numerically verify that the large- N_c prediction is valid down to $N_c = 2$ due to the large statistical error of b_2 at $N_c = 2$. In order for the large N_c theory to accommodate $b_2 = -1/48$ at $N_c = 2$, there has to be a sizable next-order corrections of $O(1/N_c^4)$; another possibility is that b_2 is a discontinuous function of $1/N_c$ between $N_c = 2$ and 3. The improved determination of b_2 will be of help in further elucidating the consistency with the large N_c predictions.

6 Summary

The sub-volume method was originally developed to estimate the θ -dependence of the free energy density to $\theta \sim O(1)$ without any expansion in [14]. In this paper this method is applied to the calculation of the topological susceptibility χ and the fourth cumulant b_2 around the critical temperature T_c . We have successfully reduced the statistical uncertainties of both quantities compared to those in the standard full-volume method. Thanks to the improvement, it is found that χ has a peak around T_c , and that b_2 behaves approximately as a constant both inside the confined and deconfined phases— b_2 in the deconfined phase is close to the instanton prediction, $-1/12$, as expected, while the one in the confined phase turns out to be consistent with $-1/48$ down to $T = 0$. From this observation, we deduced that θ -dependence of the free energy density, normalized by the topological susceptibility, in SU(2) YM theory is close to $4(1 - \cos(\theta/2))$ in the confined phase at least in the vicinity of $\theta = 0$. This proposal is consistent with the expectation that there are two meta-stable branches of the SU(2) theory, each of which has 4π periodicity [22, 24].

We are currently investigating the whole θ -dependence of the free energy density $f(\theta)$ at finite temperature. In order to understand the whole θ - T phase diagram, it is also important to study the θ -dependence of the transition temperature $T_c(\theta)$ and what happens to $f(\theta)$ when it crosses the transition line.

In our calculation with the sub-volume method, the large-sub-volume extrapolation has been performed in several different ways to estimate the systematic uncertainties. There is room for reducing the uncertainty by increasing the data points, which requires larger lattices. It is also interesting to explore the relationship between our low- T value $b_2 = -1/48$ at $N_c = 2$ and the large N_c scaling $b_2 \sim 1/N_c^2$ valid, at least, down to $N_c = 3$. We will leave those tasks to future works.

Acknowledgments

This work is based in part on the Bridge++ code [45] and is supported in part by JSPS KAKENHI Grant-in-Aid for Scientific Research (Nos. 19H00689 [RK, NY, MY], 21H01086 [RK], 22K21350 [RK], 22K03645 [NY], 19K03820, 20H05860, 23H01168 [MY]), and JST, Japan (PRESTO Grant No. JPMJPR225A, Moonshot R& D Grant No. JPMJMS2061 [MY]). This research used computational resources of Cygnus and Wisteria/BDEC-01 Odyssey (the University of Tokyo), provided by the Multidisciplinary Cooperative Research Program in the Center for Computational Sciences, University of Tsukuba.

References

- [1] C. G. Callan, Jr., R. F. Dashen and D. J. Gross, “The Structure of the Gauge Theory Vacuum,” *Phys. Lett. B* **63**, 334-340 (1976) doi: [10.1016/0370-2693\(76\)90277-X](https://doi.org/10.1016/0370-2693(76)90277-X)
- [2] B. Lucini, M. Teper and U. Wenger, “The Deconfinement transition in $SU(N)$ gauge theories,” *Phys. Lett. B* **545**, 197-206 (2002) doi: [10.1016/S0370-2693\(02\)02556-X](https://doi.org/10.1016/S0370-2693(02)02556-X) [arXiv:hep-lat/0206029 [hep-lat]].
- [3] B. Lucini, M. Teper and U. Wenger, “The High temperature phase transition in $SU(N)$ gauge theories,” *JHEP* **01**, 061 (2004) doi: [10.1088/1126-6708/2004/01/061](https://doi.org/10.1088/1126-6708/2004/01/061) [arXiv:hep-lat/0307017 [hep-lat]].
- [4] C. Bonati, M. D’Elia, H. Panagopoulos and E. Vicari, “Change of θ Dependence in 4D $SU(N)$ Gauge Theories Across the Deconfinement Transition,” *Phys. Rev. Lett.* **110**, no.25, 252003 (2013) doi: [10.1103/PhysRevLett.110.252003](https://doi.org/10.1103/PhysRevLett.110.252003) [arXiv:1301.7640 [hep-lat]].
- [5] R. Kitano, N. Yamada and M. Yamazaki, “Is $N = 2$ Large?,” *JHEP* **02**, 073 (2021) doi: [10.1007/JHEP02\(2021\)073](https://doi.org/10.1007/JHEP02(2021)073) [arXiv:2010.08810 [hep-lat]].
- [6] M. D’Elia and F. Negro, “ θ dependence of the deconfinement temperature in Yang-Mills theories,” *Phys. Rev. Lett.* **109**, 072001 (2012) doi: [10.1103/PhysRevLett.109.072001](https://doi.org/10.1103/PhysRevLett.109.072001) [arXiv:1205.0538 [hep-lat]].
- [7] M. D’Elia and F. Negro, “Phase diagram of Yang-Mills theories in the presence of a θ term,” *Phys. Rev. D* **88**, no.3, 034503 (2013) doi: [10.1103/PhysRevD.88.034503](https://doi.org/10.1103/PhysRevD.88.034503) [arXiv:1306.2919 [hep-lat]].
- [8] C. Bonati, M. D’Elia, P. Rossi and E. Vicari, “ θ dependence of 4D $SU(N)$ gauge theories in the large- N limit,” *Phys. Rev. D* **94**, no. 8, 085017 (2016) doi: [10.1103/PhysRevD.94.085017](https://doi.org/10.1103/PhysRevD.94.085017) [arXiv:1607.06360 [hep-lat]].
- [9] N. Otake and N. Yamada, “ θ dependence of T_c in 4d $SU(3)$ Yang-Mills theory with histogram method and the Lee-Yang zeros in the large N limit,” *JHEP* **06**, 044 (2022) doi: [10.1007/JHEP06\(2022\)044](https://doi.org/10.1007/JHEP06(2022)044) [arXiv:2202.05605 [hep-lat]].
- [10] S. Borsanyi, Z. Fodor, D. A. Godzieba, R. Kara, P. Parotto, D. Sexty and R. Vig, “Topological features of the deconfinement transition,” *Phys. Rev. D* **107**, no.5, 054514 (2023) doi: [10.1103/PhysRevD.107.054514](https://doi.org/10.1103/PhysRevD.107.054514) [arXiv:2212.08684 [hep-lat]].
- [11] C. Bonanno, M. D’Elia and L. Verzichelli, “The θ -dependence of the $SU(N)$ critical temperature at large N ,” *JHEP* **02**, 156 (2024) doi: [10.1007/JHEP02\(2024\)156](https://doi.org/10.1007/JHEP02(2024)156) [arXiv:2312.12202 [hep-lat]].

- [12] M. Hirasawa, K. Hatakeyama, M. Honda, A. Matsumoto, J. Nishimura and A. Yosprakob, “Determination of the CP restoration temperature at $\theta = \pi$ in 4D SU(2) Yang-Mills theory through simulations at imaginary θ ,” [arXiv:2401.05726 [hep-lat]].
- [13] C. Bonanno, C. Bonati, M. Papace and D. Vadacchino, “The θ -dependence of the Yang-Mills spectrum from analytic continuation,” [arXiv:2402.03096 [hep-lat]].
- [14] R. Kitano, R. Matsudo, N. Yamada and M. Yamazaki, “Peeking into the θ vacuum,” Phys. Lett. B **822**, 136657 (2021) doi: [10.1016/j.physletb.2021.136657](https://doi.org/10.1016/j.physletb.2021.136657) [arXiv:2102.08784 [hep-lat]].
- [15] G. 't Hooft, “A Planar Diagram Theory for Strong Interactions,” Nucl. Phys. B **72** (1974), 461 doi: [10.1016/0550-3213\(74\)90154-0](https://doi.org/10.1016/0550-3213(74)90154-0)
- [16] E. Witten, “Large N Chiral Dynamics,” Annals Phys. **128**, 363 (1980) doi: [10.1016/0003-4916\(80\)90325-5](https://doi.org/10.1016/0003-4916(80)90325-5)
- [17] G. 't Hooft, “Topology of the Gauge Condition and New Confinement Phases in Nonabelian Gauge Theories,” Nucl. Phys. B **190**, 455-478 (1981) doi: [10.1016/0550-3213\(81\)90442-9](https://doi.org/10.1016/0550-3213(81)90442-9)
- [18] E. Witten, “Theta dependence in the large N limit of four-dimensional gauge theories,” Phys. Rev. Lett. **81**, 2862-2865 (1998) doi: [10.1103/PhysRevLett.81.2862](https://doi.org/10.1103/PhysRevLett.81.2862) [arXiv:hep-th/9807109 [hep-th]].
- [19] M. Unsal, “Theta dependence, sign problems and topological interference,” Phys. Rev. D **86**, 105012 (2012) doi: [10.1103/PhysRevD.86.105012](https://doi.org/10.1103/PhysRevD.86.105012) [arXiv:1201.6426 [hep-th]].
- [20] D. Gaiotto, A. Kapustin, Z. Komargodski and N. Seiberg, “Theta, Time Reversal, and Temperature,” JHEP **05**, 091 (2017) doi: [10.1007/JHEP05\(2017\)091](https://doi.org/10.1007/JHEP05(2017)091) [arXiv:1703.00501 [hep-th]].
- [21] R. Kitano, T. Suyama and N. Yamada, “ $\theta = \pi$ in $SU(N)/\mathbb{Z}_N$ gauge theories,” JHEP **09**, 137 (2017) doi: [10.1007/JHEP09\(2017\)137](https://doi.org/10.1007/JHEP09(2017)137) [arXiv:1709.04225 [hep-th]].
- [22] M. Yamazaki and K. Yonekura, “From 4d Yang-Mills to 2d \mathbb{CP}^{N-1} model: IR problem and confinement at weak coupling,” JHEP **07**, 088 (2017) doi: [10.1007/JHEP07\(2017\)088](https://doi.org/10.1007/JHEP07(2017)088) [arXiv:1704.05852 [hep-th]].
- [23] M. Yamazaki, “Relating 't Hooft Anomalies of 4d Pure Yang-Mills and 2d \mathbb{CP}^{N-1} Model,” JHEP **10**, 172 (2018) doi: [10.1007/JHEP10\(2018\)172](https://doi.org/10.1007/JHEP10(2018)172) [arXiv:1711.04360 [hep-th]].
- [24] Y. Nomura and M. Yamazaki, “Tensor Modes in Pure Natural Inflation,” Phys. Lett. B **780** (2018), 106-110 doi: [10.1016/j.physletb.2018.02.071](https://doi.org/10.1016/j.physletb.2018.02.071) [arXiv:1711.10490 [hep-ph]].
- [25] Z. Wan, J. Wang and Y. Zheng, “New higher anomalies, SU(N) Yang-Mills gauge theory and \mathbb{CP}^{N-1} sigma model,” Annals Phys. **414**, 168074 (2020) doi: [10.1016/j.aop.2020.168074](https://doi.org/10.1016/j.aop.2020.168074) [arXiv:1812.11968 [hep-th]].
- [26] B. Lucini, M. Teper and U. Wenger, “Topology of SU(N) gauge theories at $T \simeq 0$ and $T \simeq T_c$,” Nucl. Phys. B **715**, 461-482 (2005) doi: [10.1016/j.nuclphysb.2005.02.037](https://doi.org/10.1016/j.nuclphysb.2005.02.037) [arXiv:hep-lat/0401028 [hep-lat]].
- [27] P. Keith-Hynes and H. Thacker, “Fractionally charged Wilson loops as a probe of theta-dependence in CP(N-1) sigma models: Instantons vs. large N,” Phys. Rev. D **78**, 025009 (2008) doi: [10.1103/PhysRevD.78.025009](https://doi.org/10.1103/PhysRevD.78.025009) [arXiv:0804.1534 [hep-lat]].
- [28] P. de Forcrand, M. Garcia Perez, J. E. Hetrick, E. Laermann, J. F. Lagae and I. O. Stamatescu, “Local topological and chiral properties of QCD,” Nucl. Phys. B Proc.

- Suppl. **73**, 578-580 (1999) doi: [10.1016/S0920-5632\(99\)85143-3](https://doi.org/10.1016/S0920-5632(99)85143-3) [arXiv:hep-lat/9810033 [hep-lat]].
- [29] W. Bietenholz, P. de Forcrand and U. Gerber, “Topological Susceptibility from Slabs,” JHEP **12**, 070 (2015) doi: [10.1007/JHEP12\(2015\)070](https://doi.org/10.1007/JHEP12(2015)070) [arXiv:1509.06433 [hep-lat]].
 - [30] W. Bietenholz, K. Cichy, P. de Forcrand, A. Dromard and U. Gerber, “The Slab Method to Measure the Topological Susceptibility,” PoS **LATTICE2016**, 321 (2016) doi: [10.22323/1.256.0321](https://doi.org/10.22323/1.256.0321) [arXiv:1610.00685 [hep-lat]].
 - [31] R. C. Brower *et al.* [LSD], “Maximum-Likelihood Approach to Topological Charge Fluctuations in Lattice Gauge Theory,” Phys. Rev. D **90**, no.1, 014503 (2014) doi: [10.1103/PhysRevD.90.014503](https://doi.org/10.1103/PhysRevD.90.014503) [arXiv:1403.2761 [hep-lat]].
 - [32] P. Weisz, “Continuum Limit Improved Lattice Action for Pure Yang-Mills Theory. 1.,” Nucl. Phys. B **212**, 1-17 (1983). doi: [10.1016/0550-3213\(83\)90595-3](https://doi.org/10.1016/0550-3213(83)90595-3)
 - [33] G. Cella, G. Curci, R. Tripiccion and A. Vicere, “Scaling, asymptotic scaling and Symanzik improvement. Deconfinement temperature in SU(2) pure gauge theory,” Phys. Rev. D **49**, 511-527 (1994) doi: [10.1103/PhysRevD.49.511](https://doi.org/10.1103/PhysRevD.49.511) [arXiv:hep-lat/9306011 [hep-lat]].
 - [34] P. Giudice and S. Piemonte, “Improved thermodynamics of SU(2) gauge theory,” Eur. Phys. J. C **77**, no.12, 821 (2017) doi: [10.1140/epjc/s10052-017-5392-6](https://doi.org/10.1140/epjc/s10052-017-5392-6) [arXiv:1708.01216 [hep-lat]].
 - [35] P. Hasenfratz, V. Laliena and F. Niedermayer, “The Index theorem in QCD with a finite cutoff,” Phys. Lett. B **427**, 125-131 (1998) doi: [10.1016/S0370-2693\(98\)00315-3](https://doi.org/10.1016/S0370-2693(98)00315-3) [arXiv:hep-lat/9801021 [hep-lat]].
 - [36] C. Bonati and M. D’Elia, “Comparison of the gradient flow with cooling in $SU(3)$ pure gauge theory,” Phys. Rev. D **89**, no.10, 105005 (2014) doi: [10.1103/PhysRevD.89.105005](https://doi.org/10.1103/PhysRevD.89.105005) [arXiv:1401.2441 [hep-lat]].
 - [37] C. Alexandrou, A. Athenodorou and K. Jansen, “Topological charge using cooling and the gradient flow,” Phys. Rev. D **92**, no.12, 125014 (2015) doi: [10.1103/PhysRevD.92.125014](https://doi.org/10.1103/PhysRevD.92.125014) [arXiv:1509.04259 [hep-lat]].
 - [38] C. Alexandrou, A. Athenodorou, K. Cichy, A. Dromard, E. Garcia-Ramos, K. Jansen, U. Wenger and F. Zimmermann, “Comparison of topological charge definitions in Lattice QCD,” Eur. Phys. J. C **80**, no.5, 424 (2020) doi: [10.1140/epjc/s10052-020-7984-9](https://doi.org/10.1140/epjc/s10052-020-7984-9) [arXiv:1708.00696 [hep-lat]].
 - [39] M. Albanese *et al.* [APE], “Glueball Masses and String Tension in Lattice QCD,” Phys. Lett. B **192**, 163-169 (1987) doi: [10.1016/0370-2693\(87\)91160-9](https://doi.org/10.1016/0370-2693(87)91160-9)
 - [40] P. de Forcrand, M. Garcia Perez and I. O. Stamatescu, “Topology of the SU(2) vacuum: A Lattice study using improved cooling,” Nucl. Phys. B **499**, 409 (1997) doi: [10.1016/S0550-3213\(97\)00275-7](https://doi.org/10.1016/S0550-3213(97)00275-7) [hep-lat/9701012].
 - [41] J. Frison, R. Kitano, H. Matsufuru, S. Mori and N. Yamada, “Topological susceptibility at high temperature on the lattice,” JHEP **09**, 021 (2016) doi: [10.1007/JHEP09\(2016\)021](https://doi.org/10.1007/JHEP09(2016)021) [arXiv:1606.07175 [hep-lat]].
 - [42] M. Caselle and R. Pellegrini, “Finite-Temperature Behavior of Glueballs in Lattice Gauge Theories,” Phys. Rev. Lett. **111**, no.13, 132001 (2013) doi: [10.1103/PhysRevLett.111.132001](https://doi.org/10.1103/PhysRevLett.111.132001) [arXiv:1304.4757 [hep-lat]].
 - [43] G. ’t Hooft, “Computation of the Quantum Effects Due to a Four-Dimensional

- Pseudoparticle,” Phys. Rev. D **14**, 3432-3450 (1976) [erratum: Phys. Rev. D **18**, 2199 (1978)]
[doi: 10.1103/PhysRevD.14.3432](https://doi.org/10.1103/PhysRevD.14.3432)
- [44] L. Del Debbio, H. Panagopoulos and E. Vicari, “theta dependence of SU(N) gauge theories,” JHEP **08**, 044 (2002) [doi: 10.1088/1126-6708/2002/08/044](https://doi.org/10.1088/1126-6708/2002/08/044) [arXiv:hep-th/0204125 [hep-th]].
- [45] S. Ueda, S. Aoki, T. Aoyama, K. Kanaya, H. Matsufuru, S. Motoki, Y. Namekawa, H. Nemura, Y. Taniguchi and N. Ukita, “Development of an object oriented lattice QCD code ‘Bridge++’,” J. Phys. Conf. Ser. **523**, 012046 (2014) [doi: 10.1088/1742-6596/523/1/012046](https://doi.org/10.1088/1742-6596/523/1/012046)